

Structure factors associated with melting of a $p(2 \times 2)$ ordered phase on a honeycomb lattice gas: Possible critical scattering at a first-order transition

N. C. Bartelt, T. L. Einstein, and L. D. Roelofs*

Department of Physics and Astronomy, University of Maryland, College Park, Maryland 20742

(Received 21 November 1986)

We study the order-disorder transition of a $p(2 \times 2)$ ordered state on a honeycomb lattice using Monte Carlo calculations of the structure factor. We observe a correlation length which gets large as the transition is approached; the effective critical exponents are close to the exponents characterizing a discontinuity fixed point and similar to those we observe for the first-order transition of the eight-state Potts model. We also discuss how observation of the outer integral-order diffraction beams gives information about the relevance of the field which distinguishes the two triangular sublattices of the honeycomb lattice.

I. INTRODUCTION

In this paper we discuss the results of Monte Carlo simulations of a honeycomb lattice gas which has a low-temperature $p(2 \times 2)$ phase. This structure is of particular interest because critical exponents have been measured for the disordering transition of $p(2 \times 2)$ O/Ni(111);¹ there is evidence that the binding sites of O/Ni(111) form a honeycomb lattice. There are other possible realizations of this phase in chemisorbed systems—the threefold hollows of triangular lattices [the {111} faces of fcc and bcc (and {0001} faces of hcp) single crystals] form a honeycomb lattice. There are many reports of $p(2 \times 2)$ phases occurring in systems of atoms adsorbed on these surfaces.²

Our approach has been to simulate the kinematic structure factor in selected regions of the surface Brillouin zone to get an idea of what could be observed experimentally, under ideal conditions, using low-energy electron diffraction (LEED). We used lattice sizes comparable to the sizes of defect-free regions on metallic surfaces. Further discussion on the degree to which our study resembles experiment can be found in the first paper of this series,³ hereafter called I. The lattice-gas model discussed here, however, is not a model of any particular system.

The Landau-Ginzburg-Wilson Hamiltonian classification scheme predicts that the disordering transition of this ordered state is in the same universality class as that of the Heisenberg model with corner-cubic anisotropy.⁴ Studies of this model⁵ find Ising and first-order transitions. The experimental data suggest that the transition for $p(2 \times 2)$ O/Ni(111) is Ising-like.² In order to reproduce this observation within a lattice-gas model, we tried a number of interaction sets to find a transition which was clearly second order. This attempt was unsuccessful.⁶ All the transitions studied, including the one studied here, were consistent with a first-order transition. For example, the maximum of the specific heat increased roughly as L^2 ,⁶ where L is the linear dimension of the lattices rather than as $\ln(L)$, as in the Ising model.

If the transition is first order, then it is a temperature-driven first-order transition. That is, it is the terminal point of a line of first-order transitions. As is well-

known,⁷⁻¹⁰ it can be very difficult to distinguish such a first-order transition from a second-order transition using observations on a single-sized system. (Finite-size scaling of systems over a wide range of sizes is needed, an option of course not available to experimenters.) The same problems occur in the transition studied here: the diffuse scattering has an inverse width and height which become large as the transition is approached. On the other hand, Fisher and Berker¹¹ suggest that at this type of transition, when both the magnetization and energy are discontinuous, the correlation length could diverge as $|1 - T/T_c|^{-1/2}$ and the susceptibility as $|1 - T/T_c|^{-1}$. In our study we find effective scaling and critical exponents roughly consistent with this prediction, although simulation of finite systems cannot, of course, actually determine if the correlation length diverges. Our simulations of the eight-state Potts model, which certainly has a temperature-driven first-order transition,¹² yield very similar results.

A difficult question to address experimentally is the equivalency of all the binding sites. The honeycomb net of threefold hollows can be divided into two triangular sublattices. Underlying layers of the substrate can break the symmetry of these two sublattices. It is difficult to know how significant this symmetry breaking is. Calculations of these binding energy differences for hydrogen adsorbed on transition-metal surfaces are just beginning to become reliable.¹³ In principle, it should be possible to determine whether both or just one site is occupied using LEED intensity versus voltage (I/V) analysis, although in practice there are often difficulties in doing so.¹⁴ There are also distinct differences in the disordering phase transitions between the two cases. For example, if there are no symmetry differences between the two sublattices, the $p(2 \times 2)$ ordered state spontaneously breaks the symmetry because the $p(2 \times 2)$ only occupies sites of one sublattice. As we will discuss, this shows up as a critical-like variation in some of the integer-order diffraction features.

II. DESCRIPTION OF THE MODEL

The honeycomb lattice, along with the interactions we have included in our model, is shown in Fig. 1. The in-

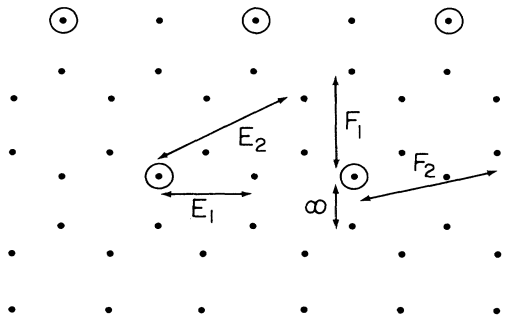


FIG. 1. The $p(2 \times 2)$ structure on a honeycomb lattice, along with the model interactions used to create it.

teractions F_0 , F_1 , and F_2 couple the two triangular sublattices composing the honeycomb lattice. F_0 was taken to be infinitely repulsive [as is probably the case when atoms adsorb on both types of threefold hollows on the (111) face of an fcc metal, for example]. All the other interactions were also repulsive. E_2 was half of E_1 , as it was in the triangular lattice gas studied in I. The interactions F_1 and F_2 were taken to be equal to E_1 and E_2 , respectively. With a chemical potential of $1.35E_1$, about $\frac{1}{8}$ of the sites were occupied near the transition. The lattice on which most of the simulations were performed was hexagonally shaped with 7776 sites. Periodic boundary conditions were assumed. Details of the Monte Carlo calculations appear in I: 10^5 to 10^6 Monte Carlo steps per site were used in computing each average.

III. MONTE CARLO DATA

Figure 2 shows the surface Brillouin zone of the honeycomb lattice along with the positions in k space where the structure factor was computed. The two-site basis necessitates computing over two Brillouin zones; the structure factor at points \bar{M} and \bar{M}' , called the inner and outer half-order beams in diffraction experiments, are not equal. For a perfect $p(2 \times 2)$ overlayer the ratio of kinematic intensities of these two points is 1:4. Moreover, point $\bar{\Gamma}'$

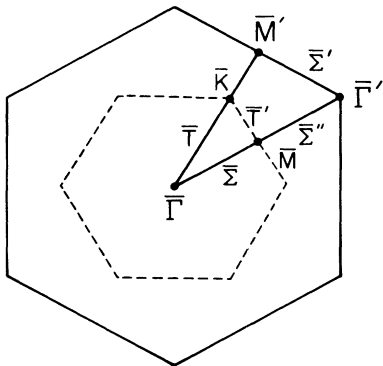


FIG. 2. The surface Brillouin zone (dashed line) and the lines along which the structure factor was computed.

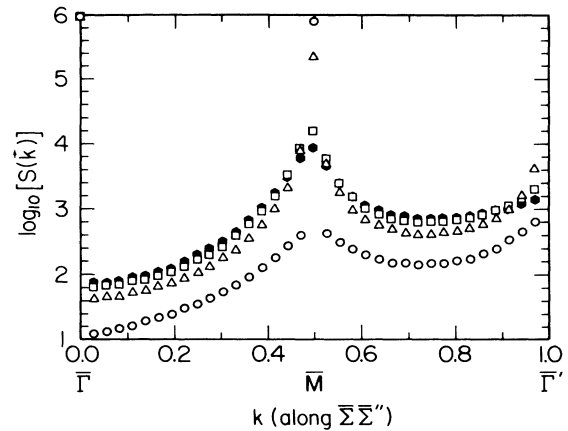


FIG. 3. The logarithm of $S(\mathbf{k})$ along the radial cut $\bar{\Gamma}\bar{M}\bar{\Gamma}'$ (i.e., $\bar{\Sigma}\bar{\Sigma}'$): $T=0.2175E_1$ (\circ), $T=0.231E_1$ (\triangle), $T=0.24255E_1$ (\square), and $T=0.255E_1$ (\bullet).

shows the effects of the order-disorder phase transition, as described in conjunction with Eq. (3) below, while $\bar{\Gamma}$ does not. Figure 3 shows a cut of the structure factor at four temperatures: approximately 5% below T_c , close to T_c , and 5% and 10% above. Figure 4 shows the temperature dependence of $S(\bar{M})$, where the structure factor is defined by

$$S(\mathbf{k}, T) = \left\langle \left| \sum_{\mathbf{r}} n(\mathbf{r}) e^{i\mathbf{k} \cdot \mathbf{r}} \right|^2 \right\rangle, \quad (1)$$

with $n(\mathbf{r})$ the occupancy (0 or 1) of the lattice site at \mathbf{r} .

IV. SCALED STRUCTURE FACTOR AND EFFECTIVE EXPONENTS

If the transition were second order, one would expect the structure factor to have the scaling form,

$$\lim_{t \rightarrow 0} \lim_{|\Delta \mathbf{k}| \rightarrow 0} S(\mathbf{k}, T) = bt^{-\gamma} X_{\pm}(at^{-\nu} |\Delta \mathbf{k}|), \quad (2)$$

where $\Delta \mathbf{k} = \mathbf{k} - \bar{M}$ and $t = |1 - T_c/T|$. Figure 5 shows

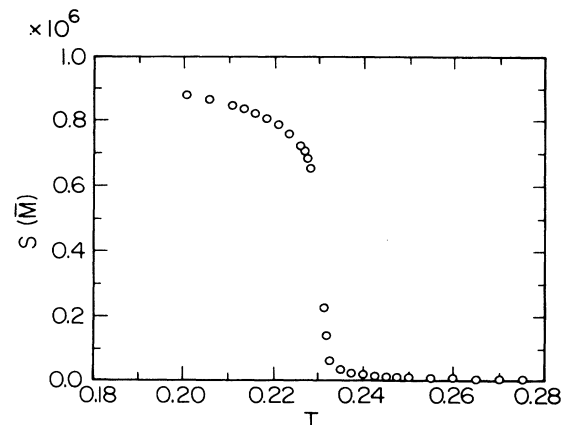


FIG. 4. The temperature dependence of $S(\bar{M})$.

some of the Monte Carlo data above T_c scaled according to this hypothesis. The exponents and T_c used are determined in the next section. The data starting about 2% away from T_c can be made to scale quite well. Notice the scaling function seems to peak at $\Delta\mathbf{k}=0$, although there is no reason by symmetry for it to do so.

The data scales over ranges of t and $|\Delta\mathbf{k}|$ similar to the continuous transitions studied in I, with finite-size effects evident below the cutoff at small t . The scaling function itself is noticeably different, however: noting $\lim_{|\Delta\mathbf{k}|\rightarrow\infty} S(\mathbf{k}) \propto |\Delta\mathbf{k}|^{-\eta-2}$ and plotting $\log(S)$ against $\log(|\Delta\mathbf{k}|)$ at T_c in the manner described in I, we obtain $\eta_{\text{eff}} \approx -0.08$, while the η_{eff} 's for the continuous transitions were positive. This observation is probably not useful experimentally because the deviations from Lorentzian-like behavior ($\eta_{\text{eff}}=0$) were so small in all cases that they would be difficult to measure.

The disordering transition of the $p(2\times 2)$ honeycomb lattice gas is more abrupt than the transitions studied in I (compare Fig. 4 with Figs. 2(f) and 3(f) in I). As discussed in the introduction, the question is whether the transition in the infinite system is first or second order. It is difficult to determine the order of a transition from simulations of a single finite-size system.⁷⁻¹⁰ One method which has been used is to examine the distributions of the square of the order parameter in the Monte Carlo simulations near the transition. These distributions were clearly double peaked for the $p(2\times 2)$ transition. However, to make the identification of order definitive one would have to study carefully the size dependence of the double-peak structure.^{10,15} Measurable quantities for this system do not behave qualitatively differently from the previous systems having continuous transitions.^{3,16} For example, as Fig. 6 explicitly shows (as does Fig. 5 implicitly), the correlation length gradually gets large as the transition is approached. Proceeding as in I, we analyze the data above $T=0.24E_1$ and below $T=0.228E_1$. This data is approximately independent of lattice size: calculations on a lattice twice the size (31,104 sites) yielded numbers consistent, within statistical errors, with Fig. 6 at tempera-

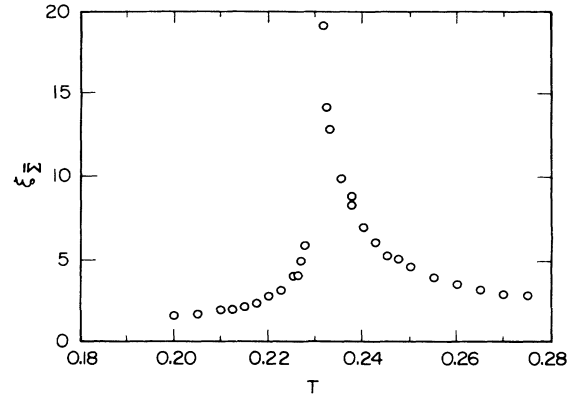


FIG. 6. Temperature dependence of the correlation length from the cut $\bar{\Sigma}$.

tures of $0.24E_1$, $0.25E_1$, and $0.26E_1$. Thus the effective exponents which we quote below are not significantly affected by the finite size of the lattice. As in I, from the structure factors we compute the susceptibility, χ [equal to $S(\bar{M})$ above T_c], the correlation length ξ , and the squared order parameter M^2 . Figure 7 shows the resulting log-log plots above T_c , from which we obtain $\gamma_{\text{eff}}=0.86\pm 0.20$, $\nu_{\text{eff}}=0.55\pm 0.15$, and $T_c^*=0.233\pm 0.004E_1$. These were the exponents and T_c used to construct Fig. 5. Below T_c corrections to "scaling" are more evident: Figure 8 shows the log-log plot of the intensity at point \bar{M} using the above estimate of the transition temperature. Also the correlation lengths are smaller below T_c . From the data below T_c , including the possibility of a nonlinear term in the thermal field (as described in I) we estimate $\gamma'_{\text{eff}}=1.0\pm 0.3$, $\nu'_{\text{eff}}=0.60\pm 0.25$, $\beta_{\text{eff}}=0.08\pm 0.03$, and $T_c=0.230\pm 0.004E_1$. Using the correlation length from \bar{MK} rather than \bar{MT} yielded roughly the same value of ν_{eff} . By fixing the exponents below T_c to be equal to the effective exponents found

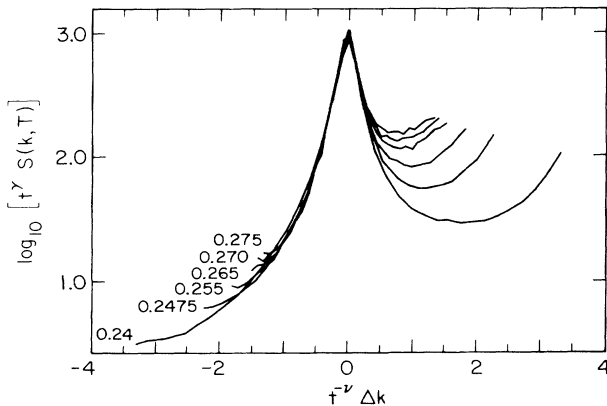


FIG. 5. Structure factors above T_c , scaled according to Eq. (2) with $\gamma=0.86$, $\nu=0.55$, and $T_c=0.233E_1$. (\mathbf{k} is along $\bar{\Sigma\Sigma}'$, with origin at \bar{M} .)

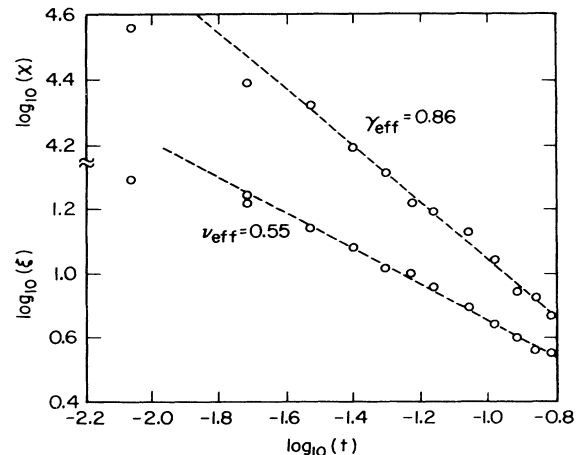


FIG. 7. Log-log plots for γ_{eff} and ν_{eff} above T_c with $T_c=0.233E_1$.

above T_c , we estimate the ratios of the susceptibility and of the correlation length above and beneath T_c , which are universal numbers in a second-order transition, to be 13_{-4}^{+11} and 1.1 ± 0.3 , respectively. These numbers are roughly a factor of 3 smaller than those observed for the lattice gases in I.

One possible explanation of this behavior was discussed in the Introduction: this transition could be first order with the order parameter and energy changing discontinuously, but with the correlation length and susceptibility diverging as T_c is approached. In this case one expects $\gamma = 1$ and $\nu = 1/d = 1/2$,¹¹ roughly consistent with the observed values of γ_{eff} and ν_{eff} . However, the correlation length of the infinite system could just get large at T_c (larger than our system size) but remain finite. In this case we would expect the effective exponents to become smaller as the system size increased above this finite value and the minimum reduced temperature used in the fit became smaller. A large but finite correlation length could be due to the proximity of a second-order transition.¹⁷ Consider, for example, the parameter space including the staggered field which distinguishes the two triangular sublattices. We know that in the limit of infinite staggered field, the case of a triangular lattice gas, the transition is second order because exactly this system was studied in I. If only a small staggered field causes the transition to become second-order, then the effects we see could be due to the closeness of our transition to the line of second-order transitions. This is possible because the same \mathbf{k} vectors (the half-order beam positions) are involved in the transition with or without the staggered field. There is nothing particularly special about the staggered field in this argument—the same role could be played by other fields which favor sets of sublattices over others. If the transition in zero (staggered) field were at a critical point

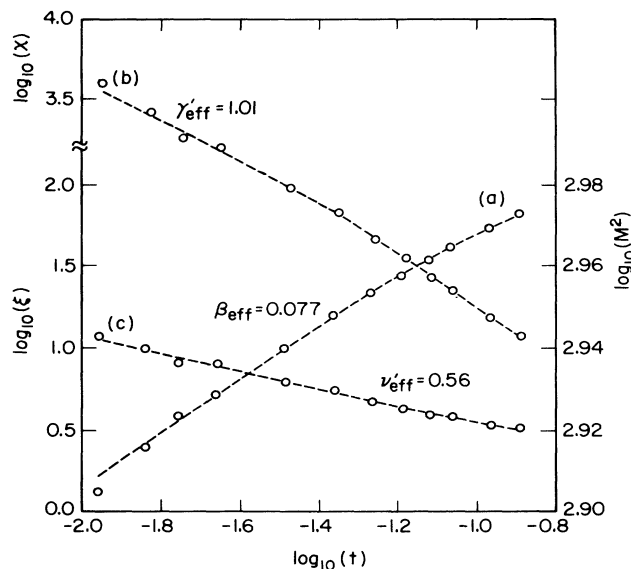


FIG. 8. Log-log plots for the effective exponents below T_c : (a) β_{eff} , (b) γ'_{eff} , and (c) ν'_{eff} . All fits include a nonlinear thermal scaling field.

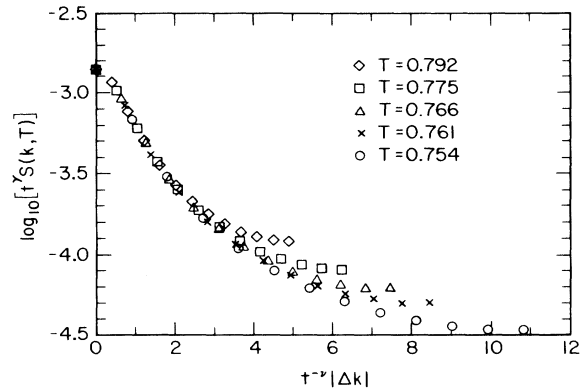


FIG. 9. Plot of the effective scaling function of the structure factor of the eight-state Potts model. Chosen to give the best scaling, γ_{eff} is 0.85, ν_{eff} is 0.6, and T_c is 0.740 [compared with T_c (exact) = 0.7449 . . .].

(second order, or first order as discussed in the preceding paragraph) then we expect the transition to be second order for all nonzero (staggered) fields¹⁸ in the neighborhood of zero staggered field.

For comparison we also performed simulations of the eight-state Potts model, which is known to have a first-order transition.¹² We observed similar behavior: a correlation length and susceptibility that get large as the transition is approached with effective exponents $\gamma_{\text{eff}} \approx 1$ and $\nu_{\text{eff}} \approx \frac{1}{2}$. Figure 9 shows the structure factor for a 24×24 square lattice Potts model scaled with $\gamma = 0.85$ and $\nu = 0.6$ and $T_c = 0.740$. [These are the parameters which gave the best scaling for data from approximately 2% to 10% above T_c . The exact T_c is 0.7449 . . . (Ref. 12).] This type of behavior has also been observed for γ_{eff} in the five- and six-state Potts models.⁹ Thus an experimenter should be wary about identifying a transition as second order exclusively on the basis of the observation of critical scattering,¹⁹ i.e., an apparently diverging peak height and inverse width.

There are effects in the structure factor of our lattice gas which have no analog in the Heisenberg model, as is

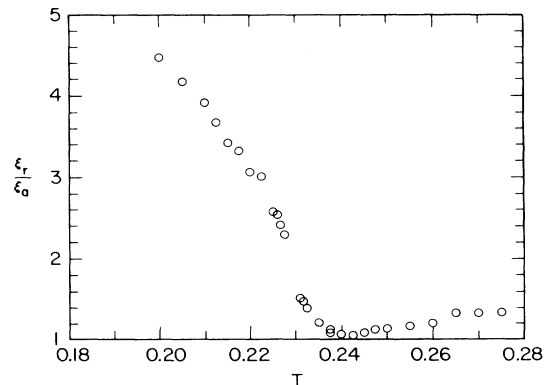


FIG. 10. Temperature dependence of the ratio of the correlation length of the inner half-order spot in the radial ($\bar{\Sigma}\bar{\Sigma}'$) and azimuthal (\bar{T}') directions with respect to $\bar{\Gamma}$.

often the case when comparing lattice-gas systems (where the translational symmetry is broken) with spin systems (where the internal spin symmetry is broken).²⁰ Figure 10 shows the temperature dependence of the ratio of the radial and azimuthal correlation length derived from an inner half-order diffraction spot: below T_c the structure factor is noticeably anisotropic. In O/Ni(111) other non-Heisenberg-model effects are seen: at coverages somewhat above $p(2 \times 2)$ saturation, the outer half-order diffraction beams are split in the disordered phase.^{21,22} Thus, caution is warranted in the identification of the behavior of this lattice gas with that of the Heisenberg model.

V. FLUCTUATION EFFECTS AT INEQUIVALENT BEAMS

As is clear from Fig. 3, the outer integral-order diffraction features in the $p(2 \times 2)$ honeycomb lattice gas (for example, point $\bar{\Gamma}'$ in Fig. 3) show the effects of critical scattering. As we will show, the intensity of the critical scattering at point $\bar{\Gamma}'$ is related to the susceptibility with respect to a field, μ_δ , which distinguishes the two triangular sublattices. The structure factor around point $\bar{\Gamma}'$ thus scales as Eq. (2) but with an exponent that may differ from that describing the scaling at $\bar{\Gamma}$. The structure factor at point $\bar{\Gamma}'$ is a measure of the difference in occupancy of the two triangular sublattices:

$$S(\bar{\Gamma}') \propto \langle \theta^2 \rangle + 3 \langle \delta^2 \rangle, \quad (3)$$

where θ is the fractional occupancy of both sublattices and δ the difference of the occupancies. The magnitude of the diffuse scattering at $\bar{\Gamma}'$ is proportional to

$$\langle \theta^2 \rangle - \langle \theta \rangle^2 + 3(\langle \delta^2 \rangle - \langle \delta \rangle^2). \quad (4)$$

The term $\langle \theta^2 \rangle - \langle \theta \rangle^2$ has a specific-heat-like singularity.²³ This term also gives the diffuse scattering at the point $\bar{\Gamma}$. Inspection of the scattering at point $\bar{\Gamma}$ in Fig. 3 shows the amplitude of this singularity is small at this coverage. At coverages away from the peak of the phase boundary, coverage fluctuations are greater. (Multiple scattering might also increase the diffuse scattering around $\bar{\Gamma}$.) Above T_c , $\langle \delta^2 \rangle$ is proportional to the susceptibility with respect to the (staggered) field μ_δ :

$$\langle \delta^2 \rangle \propto \frac{\partial^2 f}{\partial \mu_\delta^2} \propto t^{-\gamma_{\delta\delta}}, \quad (5)$$

where we have defined a new susceptibility exponent $\gamma_{\delta\delta}$. Below T_c there is a spontaneous differential occupancy of the two sublattices:

$$\lim_{\mu_\delta \rightarrow 0} \langle \delta \rangle \propto \lim_{\mu_\delta \rightarrow 0} \frac{\partial f}{\partial \mu_\delta} \propto t^{\beta_\delta}, \quad (6)$$

with $\alpha + 2\beta_\delta + \gamma_{\delta\delta} = 2$.²⁴ The crossover exponent of the field μ_δ , ϕ_δ , equals $\beta_\delta + \gamma_{\delta\delta}$. If α is smaller than $\gamma_{\delta\delta}$, the fluctuations around the point $\bar{\Gamma}'$ will be governed by critical exponents related to the application of a crystal field. Figure 11 shows the temperature dependence of $\langle \delta^2 \rangle - \langle \delta \rangle^2$ and the log-log plot for the effective exponent $\gamma_{\delta\delta}$. We conclude $(\gamma_{\delta\delta})_{\text{eff}} = 0.5 \pm 0.1$ describes the divergence of the susceptibility associated with the crystal field.

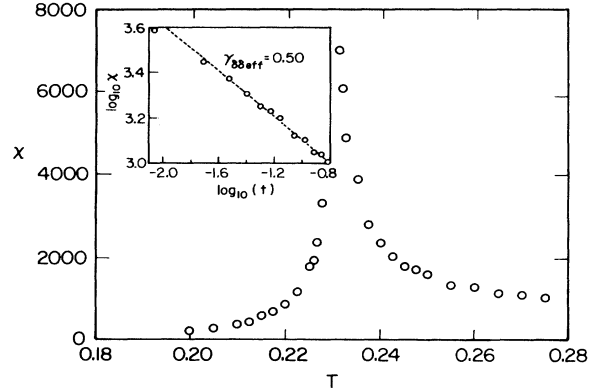


FIG. 11. Temperature dependence of the susceptibility associated with the point $\bar{\Gamma}'$ in Fig. 2. The inset shows the associated log-log plot above T_c used to determine $(\gamma_{\delta\delta})_{\text{eff}}$.

For the crossover from the Ising behavior of the Heisenberg model, Schick⁴ computes $\phi_\delta = \frac{13}{8}$, or $\gamma_{\delta\delta} = \frac{5}{4}$. (So again, we do not see Ising behavior.) In practice, observation of these critical fluctuations near $\bar{\Gamma}'$ will be difficult in general due to masking by the typically more intense substrate scattering.

This type of behavior is, of course, more general. In a typical diffraction pattern there can be many inequivalent adsorbate-induced spots which change in intensity when the adsorbate disorders. One can imagine applying a field which favors one of these diffraction features over others (e.g., the staggered field in the above discussion). The susceptibility with respect to these fields will be different for each kind of spot. If a field is a relevant perturbation, then different spots can have different exponents γ and β . By the scaling hypothesis the correlation lengths derived from each spot will diverge with the same exponent ν : there is only one diverging length scale near T_c .

There are two independent half-order spots on a honeycomb lattice: the 6 inner half-order spots (\bar{M}) have intensities different from the outer half-order spots (\bar{M}'). We do not expect their critical behavior to be different, however, because they differ by a term which couples to the coupling between the two triangular sublattices, and we expect this term to be an irrelevant perturbation at nonzero coupling. Thus the two spots would differ only in the amplitude of correction-to-scaling terms.

As another example we mention the case of the disordering of a $p(2 \times 2)$ structure on a square lattice.²⁵ The diffraction intensities around the $(\pi/a, \pi/a)$ point in k space will be different from those around $(\pi/a, 0)$. That is, the susceptibility of the system with respect to a $c(2 \times 2)$ ordering field will be different from the susceptibility with respect to a $p(2 \times 1)$ ordering field. The two diffraction features will be governed by different critical exponents because of the symmetry differences of the two fields. Interestingly, Enting suggests²⁶ that there is a universal relationship between the exponents governing the two spots: $\beta_{c(2 \times 2)} = 4\beta_{p(2 \times 2)} - \frac{1}{4}$. This difference may already have been measured for the $p(2 \times 2)$ disordering transition of S/W(110).²⁷ By the same token some diffraction features can change discontinuously at a transi-

tion while at the same time others are changing continuously (in analogy to transitions where the magnetization changes discontinuously while the energy changes continuously or vice-versa).¹¹

VI. CONCLUSION

The effective exponents we observe for our lattice-gas model of the disordering of a $p(2 \times 2)$ structure on a honeycomb lattice are much different from those observed for $p(2 \times 2)\text{O}/\text{Ni}(111)$. There are many possible explanations. One is that $p(2 \times 2)\text{O}/\text{Ni}(111)$ can be modeled by a honeycomb lattice gas, but is in a part of parameter space which has completely different "critical" behavior. If so, we have not been able to locate this region.⁶ Another possibility is that the staggered field which breaks the honeycomb lattice of binding sites into two triangular lattices is non-negligible and causes crossover effects which complicate interpretation of the experiment. As such, our model might be more appropriate as a model of adatoms adsorbed on the atop sites of graphite, for example, where

there is no staggered field.

Identifying a transition as second order just on the basis of observation of critical scattering in limited size systems (or, for that matter, of seeing no hysteresis), as is sometimes done on surfaces, is risky. It is perhaps better, as done here, to quote effective exponents.

In the $p(2 \times 2)$ lattice gas some integer-order spots can have different critical behavior from that at $\bar{\Gamma}$. Although this effect probably would not show up in LEED studies of gases on metals, because of the large substrate background, it might be observable with atom scattering or reflection high-energy electron diffraction (RHEED), which would be more surface sensitive, or in cases of heavy adsorbates on light (low- Z) substrates.

ACKNOWLEDGMENTS

This work was partially supported by the U. S. Department of Energy under Grant No. DE-FG05-84ER45071. Computer facilities, were supplied by the University of Maryland, Computer Science Center.

*Permanent address: Department of Physics, Haverford College, Haverford, PA 19041.

¹L. D. Roelofs, A. R. Kortan, T. L. Einstein, and R. L. Park, Phys. Rev. Lett. **46**, 1465 (1985).

²G. A. Somorjai, *Chemistry in Two Dimensions: Surfaces* (Cornell University Press, Ithaca, 1984).

³N. C. Bartelt, T. L. Einstein, and L. D. Roelofs, Phys. Rev. B **35**, 1776 (1987).

⁴M. Schick, Phys. Rev. Lett. **47**, 1347 (1981).

⁵G. Grest and M. Widom, Phys. Rev. B **24**, 6508 (1981).

⁶L. D. Roelofs, N. C. Bartelt, and T. L. Einstein, Phys. Rev. Lett. **47**, 1348 (1981); N. C. Bartelt, T. L. Einstein, and L. D. Roelofs, J. Vac. Sci. Tech A **1**, 1217 (1983).

⁷K. Binder and D. P. Landau, Phys. Rev. B **30**, 1477 (1984).

⁸M. S. S. Challa, D. P. Landau, and K. Binder, Phys. Rev. B **34**, 1841 (1986).

⁹K. Binder, J. Stat. Phys. **24**, 69 (1981).

¹⁰K. Binder and D. Stauffer, in *Application of the Monte Carlo Method in Statistical Physics*, edited by K. Binder (Springer, Berlin, 1984), Chap. 1.

¹¹M. E. Fisher and A. N. Berker, Phys. Rev. B **26**, 2507 (1982).

¹²F. Y. Wu, Rev. Mod. Phys. **54**, 235 (1982).

¹³J.-P. Muscat, Phys. Rev. **33**, 8136 (1986), M. S. Daw and S. M. Foiles, Phys. Rev. B **35**, 2128 (1987), and references in both. See also, L. D. Roelofs, T. L. Einstein, N. C. Bartelt, and J. D. Shore, Surf. Sci. **176**, 295 (1986).

¹⁴P. M. Marcus, J. E. Demuth, and D. W. Jepsen, Surf. Sci. **53**, 501 (1975).

¹⁵D. P. Landau and R. B. Swendsen, Phys. Rev. Lett. **22**, 1437 (1981).

¹⁶N. C. Bartelt, T. L. Einstein, and L. D. Roelofs, Phys. Rev. B **35**, 4812 (1987). In Fig. 8, the four sizes are $L = 18$ (\times), 24 (\triangle), 36 (\circ), and 72 (\square).

¹⁷M. E. Fisher (private communication).

¹⁸The analogous argument for the case of the continuous transition of three-state Potts model is given in J. P. Straley and M. E. Fisher, J. Phys. A **6**, 1310 (1973).

¹⁹For example, E. G. McRae and R. A. Malic, Surf. Sci. **161**, 25 (1985), who pronounce critical scattering "an unequivocal signature of a continuous transition."

²⁰D. A. Huse and M. E. Fisher, Phys. Rev. Lett. **49**, 793 (1983); Phys. Rev. B **29**, 239 (1984).

²¹L. D. Roelofs, Ph.D. thesis, University of Maryland, 1980.

²²A. R. Kortan and R. L. Park, Phys. Rev. B **23**, 6340 (1981).

²³Except when a region of coexistence between dense and sparse phases terminates in a multicritical point: then the leading "even" exponent does not necessarily correspond to what is normally identified with the specific heat. Cf. I. D. Lawrie and S. Sarbach, in *Phase Transitions and Critical Phenomena*, edited by C. Domb and J. L. Lebowitz (Academic, London, 1984), Vol. 9, Chap. 1.

²⁴M. E. Fisher, in *Collective Properties of Physical Systems*, edited by B. Lundqvist and S. Lundqvist (Academic, New York, 1973), p. 16.

²⁵P. Bak, P. Kleban, W. N. Unertl, J. Ochab, G. Akinci, N. C. Bartelt, and T. L. Einstein, Phys. Rev. Lett. **54**, 1539 (1985).

²⁶I. G. Enting, J. Phys. A **8**, 1681 (1975).

²⁷W. Witt and E. Bauer, Ber. Bunsenges. Phys. Chem. **90**, 248 (1986).